Journal of Thermal Science Vol.31, No.4 (2022) 1016−1022

https://doi.org/10.1007/s11630-022-1625-6 **Article ID: 1003-2169(2022)04-1016-07**

Measuring Thermal Conductivity of an Individual Carbon Nanotube Using Raman Spectroscopy

LI Pei[1], FENG Daili[1,2*], FENG Yanhui[1,2*], LIU Xiaofang[1], XIONG Mengya[1], ZHANG Xinxin[1,2], LIU Jinhui[3]

1. School of Energy and Environmental Engineering, University of Science and Technology Beijing, Beijing 100083, China
2. Beijing Key Laboratory of Energy Saving and Emission Reduction for Metallurgical Industry, University of Science and Technology Beijing, Beijing 100083, China
3. Department of Engineering Mechanics, Tsinghua University, Beijing 100084, China

Abstract: In this paper, a non-contact method based on Raman spectroscopy was used to measure the thermal conductivity of an individual single-walled carbon nanotube (SWCNT) and a multi-walled carbon nanotube (MWCNT). The effect of laser-induced heating on carbon nanotubes (CNTs) was considered. The local temperatures along the longitudinal direction of carbon nanotube were determined by Raman shift, combined with one-dimensional heat conduction model, and the thermal conductivity was finally obtained. The thermal conductivity of the SWCNT with a length of 25 μm and a diameter of 1.34 nm decreases as the temperature increases in the measuring temperature range (316 K–378 K). The corresponding thermal conductivities change from 1651 W/(m·K) to 2423 W/(m·K); the thermal conductivities of the MWCNT with 40 μm length and 9.2 nm diameter are within 1109–1700 W/(m·K) at 316 K–445 K. To further analyze the size effect on the thermal conductivity, molecular dynamics simulation has been carried out. The result shows that the thermal conductivity of an individual carbon nanotube increases with increasing nanotube length and eventually converges. This work is expected to provide some reference data for the studies of thermal properties of individual CNTs.

Keywords: carbon nanotube, thermal conductivity, Raman spectroscopy, molecular dynamics

1. Introduction

As the size of electronic devices decreases to micro even nano-scales, heat dissipation has become a critical factor limiting the progress of micro-electronics industry, therefore exploring materials with excellent thermal conductivities is rather essential. Since their discovery in 1991 [1], carbon nanotubes (CNTs) have aroused extensive attention, due to their unique thermal stability and thermal conductivity which are promising in the field of microscale heat transfer [2, 3]. Therefore, accurate thermal conductivity of CNTs is of great importance.

To date, the theoretical research on the thermal conductivity of CNTs has been relatively mature

Special issue: Nano/Microscale Heat Transfer GE: MIAO Tingting
Received: Feb 10, 2021
Corresponding authors: FENG Daili; E-mail: dlfeng@ustb.edu.cn
FENG Yanhui yhfeng@me.ustb.edu.cn

attributed to the widely used molecular dynamics modeling. From aspect of experimental measurements, due to the extremely small feature size of CNTs, it is difficult to obtain the thermal conductivity by conventional thermal measuring techniques. In recent years, researchers have developed steady-state heat flow methods [4], 3ω method [5], T-type method [6], Raman spectroscopy [7], etc. to measure thermal conductivity of individual CNTs. However, the results derived from different experimental methods are controversial and much lower than theoretical prediction. The steady-state heat flow method and 3ω method are characterized by easy operation and reasonable accuracy. But a clear linear relationship between electrical resistance of the sample and temperature is required, thus the universality is limited. T-type method applies indirect temperature measurement using platinum resistance; additional thermal resistance makes the measurement more complicated and difficult to carry out. While Yue [8–10] carried out a series of work to measure the thermal conductivity of MWCNTs and buckypapers using the steady-state electro-Raman thermal technique, which is simple and fast by further improving the technique and only considering the heating effect from the laser. In addition, Li [7] measured the thermal conductivity of an individual CNT by the Raman method, but the absorptivity of CNT to the laser needs to be obtained first. Zhang's group [11] later developed a new method for measuring the thermal conductivity and contact thermal resistance of one-dimensional micro/nanowires. This method has been successfully applied in the thermal conductivity measurement of carbon fiber without absorptivity.

In this work, the thermal conductivity of an individual CNT was measured by Raman spectroscopy proposed by Zhang [11]. The heating effect of laser on CNTs was taken into account. The measurement of suspended individual CNT with different electric heating power was carried out under certain laser heating power. The work is expected to provide some reference data and experimental basis for the thermal conductivity of individual CNTs.

2. Theoretical Basis

2.1 Physics model

The diameter of individual CNTs measured in this experiment ranges from a few nanometers to several tens of nanometers, thus micro devices are used as a carrier for measurement. The schematic diagram is shown in Fig. 1. The silicon wafer with SiO_2 oxide layer is used as the substrate. An individual CNT is designed to be suspended on the silver conductive adhesive heat sink at two ends. The initial temperature of the base channel is maintained at T_0 (K). The experiment is carried out in a vacuum environment, and the contact portions between the two ends of the CNT and the substrate are adhered by silver conductive adhesive and serve as electrodes. The direct current passed through CNTs from the silver adhesive and the voltage U (V) at both ends is measured. At the same time, the center point O of the CNT is heated by the green laser with a wavelength of 514.5 nm where the distance between the heating points and the heat sink on both sides is l (m).

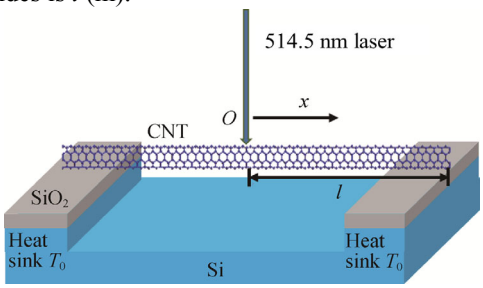

Fig. 1 Schematic diagram of the experiment setup

2.2 Calculation principle of thermal conductivity

Since the radial heat conduction of CNTs can be negligible compared to axial heat conduction, we assume that the heat transfer in CNTs meets one-dimensional heat conduction model. When the temperature of the CNTs reaches steady state, the heat conduction differential equation is as follows:

$$\frac{\mathrm{d}^2T}{\mathrm{d}x^2}+\frac{P_\mathrm{e}/2}{\lambda Al}=0 \tag{1}$$

where λ is the thermal conductivity of the CNT (W/(m·K)); T is the temperature of the sample (K); $P_\mathrm{e}=(UI)_\mathrm{CNT}=(U^2/R)_\mathrm{CNT}$ is the electric heating power at two ends of the CNT (W); R_CNT is the resistance (Ω); $A=\pi db$ is the heat transfer area (m^2) of the annular CNT; d is the diameter (m), and b is the thickness of the CNT cross section ring (m) .

Considering the symmetry of the system, we analyze the test structure using half of the volume. The boundary conditions are:

$$\begin{cases}-\lambda\left.\dfrac{\mathrm{d}T}{\mathrm{d}x}\right|_{x=0}=\dfrac{P_\mathrm{l}/2}{A}\\ T\big|_{x=l}=T_0\end{cases} \tag{2}$$

where P_l is the absorbed laser power of CNT (W). Bringing the boundary conditions into Eq. (1), we can get the temperature distribution along the length of the CNT:

$$T(x)=-\frac{P_\mathrm{e}}{4\lambda Al}x^2-\frac{P_\mathrm{l}}{2\lambda A}x+T_0+\frac{P_\mathrm{e}l+2P_\mathrm{l}l}{4\lambda A} \tag{3}$$

Further, the temperature at the center of the sample is obtained as follow:

$$T\big|_{x=0}=T_0+\frac{P_\mathrm{e}l+2P_\mathrm{l}l}{4\lambda A} \tag{4}$$

Keeping the laser heating power fixed, changing the power supply, and ignoring the change of the thermal conductivity of the carbon nanotube in the process, the temperature difference at the center point of the CNT under two different electric power conditions can be obtained as:

$$\Delta T = \frac{\Delta P_e l}{4\lambda A} = \frac{\Delta\left(U^2/R\right)_{\mathrm{CNT}} l}{4\lambda A} \tag{5}$$

where ΔP_e is the variation of the power supply. Finally, the thermal conductivity of the CNT can be described as:

$$\lambda = \frac{\Delta\left(U^2/R\right)_{\mathrm{CNT}} l}{4A\Delta T} \tag{6}$$

3. Experimental

The Laser Raman measurement platform in the experiment is from Professor ZHANG Xing's laboratory. It mainly includes optical measurement system, electrical measurement system, vacuum system and temperature control system [11]. Firstly, due to the small size of the CNTs, a vacuum system was used to isolate the air during the measurement process, thereby eliminating the effect of convective heat transfer. In addition, the damping design of vacuum system can prevent the vibration of the sample stage from affecting the laser irradiation point and causing the scattered signal to be unstable. The Raman signal was excited by green laser with a wavelength of 514.5 nm, which was generated by a spectroscopic physical model stabilized 2018 ion laser. The signal was focused on the sample by an objective lens with a magnification of 50× long working distance (LWD) and a numerical aperture of 0.5. Furthermore, the Linkam THMS600 temperature control platform can achieve an accuracy of 0.1 K.

The micro-device pattern was designed by L-edit software and 5–100 μm unequal-width micro-grooves were engraved on the substrate by photolithography. The

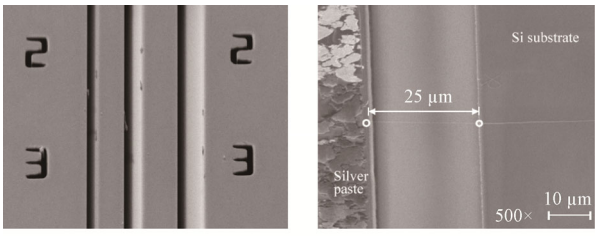

(a) Trenches (b) Suspended SWCNT

Fig. 2 SEM image of trenches and nanotube

sample was grown by chemical vapor deposition (CVD) method [12]. Under the gas flow, the CNTs were grown across the trough. Fig. 2(a) shows the Scanning Electron Microscope (SEM) image of the design layout. The mark of the channel edge is the positioning number designed for easy measurement. Fig. 2(b) is the image of microgroove after the growth of suspended CNT. The actual length of the sample was measured to be 25 μm.

4. Results and Discussion

4.1 Determination of CNT diameter

Experiment was carried out for SWCNT with a length of 25 μm. The reference temperature of 300 K was selected and a laser power of 0.5 mW was applied. Radial Breathing Mode (RBM) has a peak value of 166.7 cm^{-1}, which is a unique feature of SWCNTs [13]. It is sensitive to diameter. Studies have shown that the correlation between RBM peak and diameter can be expressed as d=227/ω_{RBM} [14]. Therefore, the diameter of SWCNTs is 1.36 nm in this paper.

For MWCNT, due to the interaction between different tube walls, no obvious breathing mode can be detected during the measurement. So the exact value of the diameter cannot be obtained according to the formula. Therefore, a Transmission Electron Microscope (TEM) was employed to measure the diameter of MWCNT of which is 9.2 nm (Fig. S1). And the actual length of the MWCNT sample is 40 μm measured by SEM (Fig. S2).

4.2 Determination of CNT electric resistance

Due to the limitation of preparation method, a couple of CNTs grown in a suspended manner are generally obtained at the same time. In order to measure an individual CNT, the following treatment is required: a couple of CNTs between the two silver adhesives electrodes are regarded as multi-resistors in parallel. Firstly, we measure the total resistance R_1 of CNTs obtained between the two electrodes. Then we use the Focused Ion Beam (FIB) to cut off individual CNT which has finished Raman measuring, and the total resistance R_2 between the electrodes is tested again. Finally, the resistance of the CNT sample can be calculated according to the parallel relationship equation (7).

$$\frac{1}{R_1} = \frac{1}{R_{\mathrm{CNT}}} + \frac{1}{R_2} \tag{7}$$

In our experiment, the R_1 of multiple parallel SWCNTs is 4.47×10^6 Ω and R_2 is 6.24×10^6 Ω. The calculated sample resistance R_{CNT} is 1.57×10^7 Ω. Similarly, the resistance of MWCNT sample R_{CNT} is derived to be 2.82×10^5 Ω.

4.3 Relationship between CNT *G*-peak position and temperature

Previous experiments have shown that the Raman *G* peak of CNT exhibits linear correlation with the

temperature [15, 16]. In this work, shift-temperature relationship on *G* band Raman spectra was measured. As shown in Fig. 3, the intensity of the *G* band Raman spectra at different temperatures does not change significantly by controlling the focus of the laser. Therefore, it is believed that the heating of the CNT by the laser is consistent. As the temperature increases within the calibration temperature range of 300 K–500 K, the peak position of the *G* band Raman spectra shifts toward the direction of low wavenumber. The *G*-band frequencies of SWCNT at different temperatures are shown in Fig. 4. The uncertainty in the measurement is 0.15 cm^{-1}. The fitting expression is $G=-0.02T+1589.5$, where the slope of the fitted line is the temperature coefficient of the *G* peak shift. In this experiment, the temperature dependency coefficient of *G* band frequency for SWCNT is 0.02 $cm^{-1}\cdot K^{-1}$, which means, there is a 50 K temperature difference for every wavenumber shift. Using the same measurement method, the formula of *G* peak variation with temperature for MWCNT is $G=-0.023T+1588.31$, similarly, every wavenumber shift corresponds to a 43.5 K temperature change.

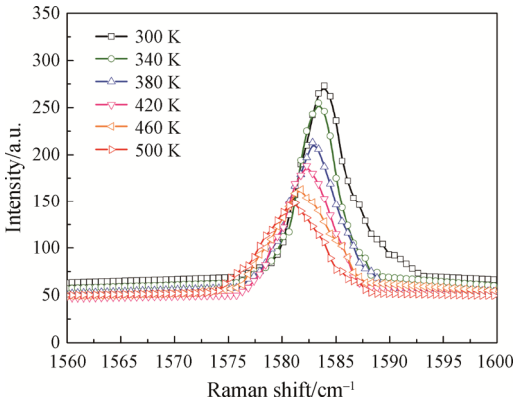

Fig. 3 *G*-peaks at the center of SWCNT at different temperatures

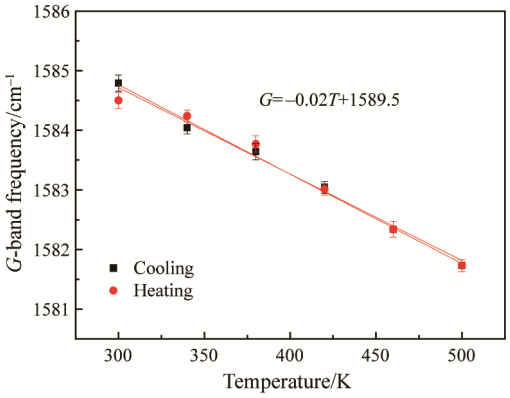

Fig. 4 *G*-band frequencies of SWCNT at different temperatures

To investigate the influence of temperature change on the Raman spectrum of CNT, heating-cooling process was conducted, and the *G*-peak shifting remained stable. Actually, due to the uneven CNT samples, the sensitivity of the Raman signals to temperature would be non-identical induced by different samples or different positions. In the experiment, the fitting error is reduced by repeating the measurements. We obtained that the *G*-peak shifts by one wavenumber and the corresponding temperature change range is 40 K–50 K. The results are basically consistent with the previous researches [15, 17].

4.4 Results of thermal conductivity measurement

The temperature rise was obtained according to the *G* band frequency in the middle part shift. The voltage, resistance and size of the tested CNT have been obtained. The thermal conductivity can be finally calculated by Eq. (6). The heating power varies with the voltages, thus, the average temperature of CNT is different. When the current is 1 V, the thermal conductivity of SWCNT is (2170±280) W/(m·K) at the average temperature of 316 K (Fig. S3).

For the MWCNT measured in this paper, on the one hand, the conductivity is slightly better than that of SWCNT; on the other hand, the higher voltage measurement will cause a large change in resistance with the length increasing. The low voltage was adopted to ensure the accuracy of measurement. When the current is 1 V, the thermal conductivity of MWCNT is (1500±270) W/(m·K) at the average temperature of 316 K. Compared with SWCNT, we used the entire cross-section instead of the ring while calculating the thermal conductivity of MWCNT. The relationship between the calculated thermal conductivity and average temperature is described in Fig. S4. As the temperature increases, the thermal conductivity of both SWCNT and MWCNT decreases (Fig. S4).

To verify the experimental results, the thermal conductivity of CNTs was further simulated by Equilibrium Molecular Dynamics (EMD) and Nonequilibrium Molecular Dynamics (NEMD). The physical model established in this paper is consistent with the experimental model. The chirality of the SWCNT was determined to be (11, 9) spiral by comparison with the Kataura [18] diagram. For MWCNT, the number of layers of the tube wall cannot be accurately distinguished in the experiment, and MWCNT does not have a Raman breathing mode, so the chirality cannot be accurately determined. Nasir [19] found that there is almost no difference in the thermal conductivity of CNTs with different chiralities under the same diameter, which proves that the thermal conductivity has little relationship with the chirality index. In this paper, the MWCNT close to the experimental diameter and a

common chirality is used as an example for simulation calculation. The AIREBO potential function [20] was used in the simulation. To reduce the size effect, the tube axial direction adopts periodic boundary condition while the circumferential direction with free boundary condition. The result is shown in Fig. 5.

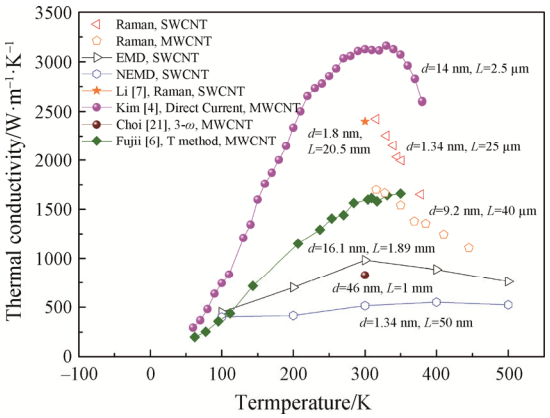

Fig. 5 Temperature dependence of CNTs' thermal conductivity [4, 6, 7, 21] (d is the diameter of CNTs, and L stands for the length of CNTs.)

For further verification, Fig. 5 also represents experimental results of the literature. Li [7] adopted Raman spectroscopy to measure SWCNT with similar dimensions and obtained the thermal conductivity of (2400±400) W/(m·K) at 300 K which is close to our results, that is, the measurement methods and results in this paper are reliable. Choi [21] measured the thermal conductivity of MWCNT at 300 K by 3-ω method, and the value is 830 W/(m·K). Kim [4] conducted a power measurement on MWCNT with a length of 2.5 μm and a diameter of 14 nm by means of the design of the micro device. It was found that the thermal conductivity of CNTs reached a maximum at around 300 K and the measured value was higher than the result of Raman method at the same temperature. Fujii [6] measured the thermal conductivity of double-walled CNT by T-method and found that the thermal conductivity also increases with the increase of temperature between 100 K and 300 K. The measurement results of Fujii and Choi are lower than other experimental values. It is mainly due to their large diameter and short length of the CNTs. Although the measurement methods are different, the variation trend between thermal conductivity and temperature is consistent. More thermal phonons are excited with temperature increase under 300 K, which contributes to a significant increase of the thermal conductivity. When the temperature is above 300 K, more phonon scattering is induced and the thermal resistance is increased, which results in the suppression of heat flow and decrease of thermal conductivity.

To analysis the effect of axial length, this paper simulates SWCNT with different lengths. As indicated in Fig. 6, our results are close to the simulation values of Lukes [22], Maruyama [23], Hou [24], Alaghemandi [25] and etc.The trends are basically the same, which verifies the reliability of the results. Wang [26] used the wave vector (WV) model of phonon conduction to predict the thermal conductivity of CNTs. The boundary scattering effect of phonons was neglected in the simulation, which resulted in a higher value compared to this paper. In summary, different simulation methods (EMD, NEMD) and potential functions (AIREBO, REBO, Brenner, etc.) influence the values of thermal conductivity, however, the trend is consistent, that is, all increase with the tube length increase. Limited by the amount of calculation, the length of the CNT set in this simulation is short. The phonon is still in the ballistic transport state, that is, the effect of scattering between phonons is negligible and the boundary scattering is dominant in the heat transfer process. Thus the thermal conductivity value is less than that of micron.

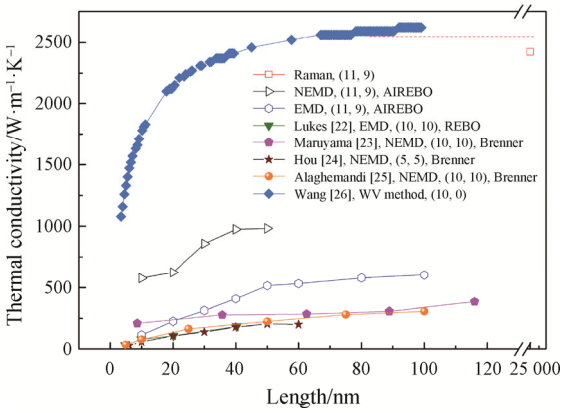

Fig. 6 Length dependence of SWCNT's thermal conductivity [22–26]

4.5 Error analysis

Experimental error in this paper comes from radiant heat and temperature measurement. Firstly, considering the influence of radiant heat, the maximum value of radiation power is: $P_{\text{radiation}}=\sigma(T^4-T_0^4)\pi dl=2.75\times10^{-10}$ W. The heating power of the laser is 0.5 mW without direct current. According to Wang [27], the absorbed laser power of the CNTs only accounts for about 0.2%, and the heat absorbed from the laser is: $P_l=0.5\times10^{-3}\times0.2\%=1\times10^{-6}$ W. When direct current is applied, the minimum electric heating power in the experiment is $P_e=UI=5.82\times10^{-8}$ W. It is indicated that radiant heat is negligible compared to laser and electric heating. Therefore, experimental error mainly comes from temperature measurement. The uncertainty of the Raman G peak position during the fitting process is 0.15 cm^{-1}.

According to shift-temperature relationship on G band Raman spectra, temperature error caused by this uncertainty is 0.15 cm^{-1}×50 K/cm^{-1}=7.5 K, which resulted in a maximum error ΔT of 15 K. Moreover, the maximum deviation of the G peak at center point is 1.2 cm^{-1}, and the measured temperature error is 1.20 cm^{-1}×50 K/cm^{-1}= 60 K; thus, the relative error $\delta(T)$ is 25%. If the other parameter except for temperature in Eq. (6) is regarded as constant, the maximum error $\delta(\lambda)$ of the thermal conductivity obtained by the error transfer formula is 25%. In the experiment, the error from peak frequency fitting can be reduced by measuring the mean value of G peak and extending the scanning time, etc. The measurement error of the single-wall and multi-wall sample is about 13% and 18%, respectively.

5. Conclusions

In the current study, the thermal conductivity of SWCNT and MWCNT were determined by Raman spectroscopy, and the measured results were compared with molecular dynamics simulation values and literature experimental values.

The conclusions are as follow: (1) The thermal conductivity of SWCNT (length 25 μm, diameter 1.36 nm) is 1651–2423 W/(m·K) at 316 K–378 K while the thermal conductivity of the MWCNT (length 40 μm, diameter 9.2 nm) is 1109–1700 W/(m·K) at 316 K–445 K. The thermal conductivity decreases with increasing temperature. (2) The measurement error of SWCNT and MWCNT is about 13% and 18%, respectively. (3) The thermal conductivity has a size effect, which increases with the increase of the tube length and tends to converge. Molecular dynamics simulation value is smaller than the experimental measurement value because the length of simulated CNTs is smaller than that of the experimental sample. Heat conduction is mainly in the state of ballistic transport, and the simulated thermal conductivity is far from the convergence value.

Acknowledgments

Thanks for the support provided by the Beijing Natural Science Foundation (No. 3192022), and National Natural Science Foundation of China (No. 51876007 and No. 52176054).

References

[1] Iijima S., Helical microtubules of graphitic carbon. Nature, 1991, 354(6348): 56–58.

[2] Zhang Y.F., Fan A.R., An M., et al., Thermal transport characteristics of supported carbon nanotube: Molecular dynamics simulation and theoretical analysis. International Journal of Heat and Mass Transfer, 2020, 159: 120111.

[3] Fan A.R., Hu Y.D., Zhang Y.F., et al., Preparation and water flow velocity measurement of a large diameter single-wall carbon nanotube. Nano Futures, 2021, 5(1): 015003.

[4] Kim P., Shi L., Majumdar A., et al., Thermal transport measurements of individual multiwalled nanotubes. Physical Review Letters, 2001, 87(21): 215502.

[5] Lu L., Yi W., Zhang D.L., 3 omega method for specific heat and thermal conductivity measurements. Review of Scientific Instruments, 2001, 72(7): 2996–3003.

[6] Fujii M., Zhang X., Xie H.Q., et al., Measuring the thermal conductivity of a single carbon nanotube. Physical Review Letters, 2005, 95(6): 65502.

[7] Li Q., Liu C., Wang X., et al., Measuring the thermal conductivity of individual carbon nanotubes by the Raman shift method. Nanotechnology, 2009, 20(14): 145702.

[8] Yue Y.A., Huang X.P., Wang X.W., Thermal transport in multiwall carbon nanotube buckypapers. Physics Letters A, 2010, 374(40): 4144–4151.

[9] Yue Y.A., Eres G, Wang X.W., et al., Characterization of thermal transport in micro/nanoscale wires by steady-state electro-Raman-thermal technique. Applied Physics A, 2009, 97(1): 19–23.

[10] Li M., Yue Y.A., Raman-based steady-state thermal characterization of multiwall carbon nanotube bundle and buckypaper. Journal of Nanoscience and Nanotechnology, 2015, 15(4): 3004–3010.

[11] Liu J., Wang H., Ma W., et al., Simultaneous measurement of thermal conductivity and thermal contact resistance of individual carbon fibers using Raman spectroscopy. Review of Scientific Instruments, 2013, 84(4): 44901.

[12] Zheng L.X., O'Connell M.J., Doorn S.K., et al., Ultralong single-wall carbon nanotubes. Nature Materials, 2004, 3(10): 673–676.

[13] Rao A.M., Richter E., Bandow S., et al., Diameter-selective Raman scattering from vibrational modes in carbon nanotubes. Science, 1997, 275(5297): 187–191.

[14] Araujo P.T., Maciel I.O., Pesce P.B.C., et al., Nature of the constant factor in the relation between radial breathing mode frequency and tube diameter for single-wall carbon nanotubes. Physical Review B, 2008, 24(77): 241403.

[15] Zhang Y., Xie L., Zhang J., et al., Temperature coefficients of Raman frequency of individual single-walled carbon nanotubes. The Journal of Physical Chemistry C, 2007, 111(38): 14031–14034.

[16] Zhang Y., Son H., Zhang J., et al., Laser-heating effect on Raman spectra of individual suspended single-walled carbon nanotubes. The Journal of Physical Chemistry C,

2007, 111(5): 1988–1992.
[17] Zhang X., Yang F., Zhao D., et al., Temperature dependent Raman spectra of isolated suspended single-walled carbon nanotubes. Nanoscale, 2014, 6(8): 3949–3953.
[18] Kataura H., Kumazawa Y., Maniwa Y., et al., Optical properties of single-wall carbon nanotubes. Syntheticmetals, 1999, 103(1): 2555–2558.
[19] Nasir Imtani A., Thermal conductivity for single-walled carbon nanotubes from Einstein relation in molecular dynamics. Journal of Physics and Chemistry of Solids, 2013, 74(11): 1599–1603.
[20] Stuart S.J., Tutein A.B., Harrison J.A., A reactive potential for hydrocarbons with intermolecular interactions. The Journal of Chemical Physics, 2000, 112(14): 6472–6486.
[21] Choi T.Y., Poulikakos D., Tharian J., et al., Measurement of thermal conductivity of individual multiwalled carbon nanotubes by the 3-ω method. Applied Physics Letters, 2005, 87(1): 13108.
[22] Lukes J.R., Hongliang Z., Thermal conductivity of individual single-wall carbon nanotubes. Journal of Heat Transfer, 2007, 129(6): 705–716.
[23] Maruyama S., A molecular dynamics simulation of heat conduction of a finite length single-walled carbon nanotube. Microscal Thermophysical Engineering, 2003, 7(1): 41–50.
[24] Hou Q.W., Cao B.Y., Guo Z.Y., Molecular dynamics study on thermal conductivity of carbon nanotubes. Heat Transfer-Asian Research, 2010, 39(7): 455–459.
[25] Alaghemandi M., Algaer E., Böhm M.C., et al., The thermal conductivity and thermal rectification of carbon nanotubes studied using reverse non-equilibrium molecular dynamics simulations. Nanotechnology, 2009, 20(11): 115704.
[26] Wang Z.L., Liang J.G., Tang D.W., Experimental and theoretical study of the length-dependent thermal conductivity of individual single-walled carbon nanotubes. Acta Physica Sinica, 2008, 57(6): 3391–3396.
[27] Wang H.D., Zhang X., A method for simultaneously measuring the laser absorptivity and thermal conductivity of a single micro/nano wire. Patent CN102944573B, 2014. (in Chinese)

Supporting Information

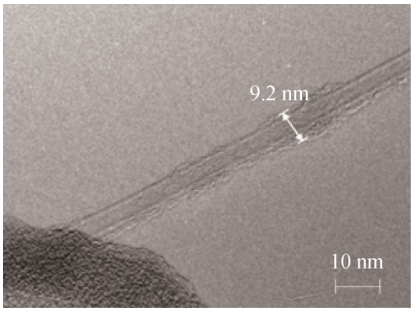

Fig. S1 TEM image of MWCNT

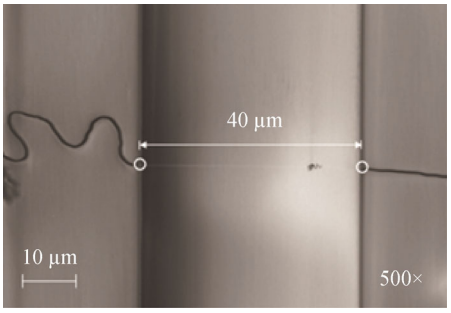

Fig. S2 SEM image of MWCNT

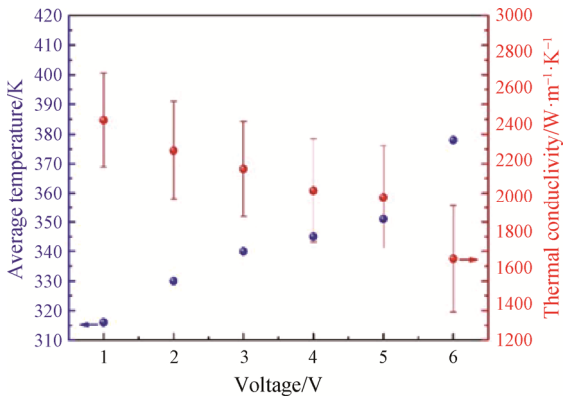

Fig. S3 Average temperature and thermal conductivity of the SWCNT (L=25 μm, D=1.36 nm) at different voltages

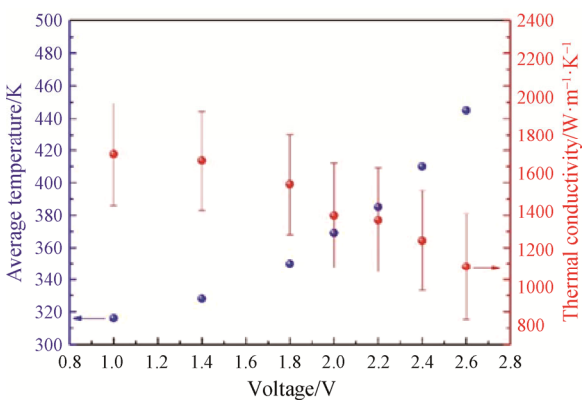

Fig. S4 Average temperature and thermal conductivity of the MWCNT (L=40 μm, D=9.2 nm) at different voltages